Physical mechanisms behind the wet adhesion: From amphibian toe-pad to biomimetics

Meng Li [a,b,c], Liping Shi [a,b,c,*], Xiaolei Wang [d,**]

[a] *School of Mechanical Engineering, Anhui University of Technology, Ma'anshan, 243032, China*
[b] *International Science and Technology Cooperation Base for Intelligent Equipment Manufacturing in Special Service Environment, Ma'anshan, 243032, China*
[c] *Anhui Province Key Laboratory of Special and Heavy Load Robot, Ma'anshan, 243032, China*
[d] *College of Mechanical & Electrical Engineering, Nanjing University of Aeronautics & Astronautics, Nanjing, 210016, China*

ABSTRACT

Some amphibians, such as tree frogs, torrent frogs, newts, are able to climb or attach to wet slippery smooth surfaces, even in a vertical or overhanging state, by their reliable reversible adhesions developed on the epidermal of toe pads. It is widely believed that such outstanding function originates from the possible factors of the specialized evolutions of surficial micro/nanostructures, the chemical components of secreted mucus, the solid-liquid behavior of epidermal and the bulk softness of toe pads. In this review, we summarize the main physical mechanisms of these factors behaving underlying the wet adhesion of toe pads from the researches on biological models to artificial counterparts. The discussion of the organism attachments, the interfacial physical forces and the switchable strategies for artificial wet adhesion are also included. The paper gives a deeply, comprehensively understanding of the characters of wet adhesives on amphibians, which performs necessarily for the new strategies of exploring artificial adhesive surfaces.

1. Introduction

The epidermal of organisms in nature which possess the extraordinary adhesions, such as walking on the ceiling or hang upside down on wet substrates, endowed by their near-surface architectures always impress us deeply. One such example is the fibrillar surface of gecko toe pads [1,2], which impose a strong but switchable role in the adhesion to almost any dry surface [3]. Experimental evidence has suggested that the gecko toe pad is composed of hundreds of thousands of keratinous hairs (called setae), which then branches into hundreds of even finer hairs (called spatula) [4,5]. With these hierarchically organized structures, the toe pads can maximize the van der Waals interaction to substrates by the intimately contacting [6,7]. Those adhesive features provide a great idea for novel surface designing [8–11].

Apart from the fibrillar surface of geckos, nature also provide a number of biological organisms with intelligent structures for facilitating strong adhesion associated with high friction under wet conditions. Amphibians such as tree frogs, torrent frogs, and newts whose toe pads usually patterned with a polygonal topography of epidermal cells separated by mucus-filled channels give great talents of attaching to

vertical and overhanging wet surfaces without slipping or falling (Fig. 1) [12–15]. As detailly investigated in previous work, these amphibian toe pad surfaces are super-hydrophilic [16] and, thus, a very thin layer of fluid always comes between the toe pads and the adhering substrates [17], which means the adhesive mechanism is quite different from geckos' case. It is generally assumed that the adhesive forces arise from the capillary forces and rate-dependent viscous forces, and that the of van der Waals forces has a probable contribution because of the several nanometers of film thickness, but to what extent is unclear [18–20]. The physical properties of toe pads, such as the surficial structures [21,22], elasticity modulus [23], hydrophilicity [16,24], *etc.*, have been demonstrated to play a positive role for the living body wet attachments. For example, the array of specialized polygonal designs of cells is suggested to have a "draining effect" that the surplus water will be removed out of the pad contact area, allowing an intimate contact situation [17, 25]. It favors producing a high friction force for the amphibian attachments when climbing on the incline slip surface [16,24,26]. In addition, other celebrated approaches to the wet adhesion such as the suction effect or the chemical interactions found on the marine organisms also gain much attentions, and have been widely reported [27–29].

Motivated by the wide range of technological application, such as climbing robot feet [10,30], novel gripper [31,32], pick-place system [33,34], etc., many researchers devote to fabricating the artificial structured surfaces for copying the super adhesive properties of living organisms, and more than one thousand articles have been published in the field over last two decades, especially for the gecko inspired fibrillary surfaces. Some of them are excellent reviews that have well discussed and systematically summarized the dry adhesion system including the underlying mechanism, the fabricating approaches, and the engineering applications, e.g., refs [9,11,35,36]. However, considering the possible case of artificially executing adhesions or bondings happening under a wet condition, the amphibians' epidermal adhesive technology, similarly, apply many potential uses for us. Obvious examples of them are improved wet weather tires, nonslip footwear, plaster for surgery able to adhere to tissue, and holding devices for neurosurgery or MEMS device. As a result, it seems necessary to give a comprehensive overview of the physical principles underlying the toe-pad wet adhesions from biological models to artificial counterparts, directing and inspiring us to carry out wide engineering applications.

This article aims to review the current state of toe pad adhesive studying, with the certain perspective of fundamental physical principles from a detailed understanding of microstructures, to tunable strategy of capillary forces. We first provide a short overview of the fascinating ability of wet attachments tested on the amphibian toe-pads (section 2). Section 3 covers the various surficial structures for wet adhesion and friction behaviors from biological epidermis structures to their biomimetics, and discussing the physical mechanisms behind them. In section 4, we reported the bulk softness, the secreted mucus, the sandwiched film in the contacts of tree frog toe-pad, providing further insights into the wedged film stability, wetting case, the bulk visco-elastic dissipation for the interfacial adhesive contacts. Section 5 reports some novel approaches to tune capillary forces between two solids for a controllable wet adhesion. A summary and future perspectives conclude the paper in Section 6.

2. The ability of wet attachments of toe-pads and their physical forces

Experimental tests on the biological organisms (Fig. 1) not only reliably verify the attachment of amphibians but also show that abilities quantitatively in a scientific way. Barness's group have a pioneering work on the measurements of the tree frog attachment ability. Their

early work were performed on Osteopilus septentrionalis (tree frog) using a force platform, showing the largest measurable adhesive forces of toe pads is about 1.2 mN mm^{-2} [37]. The climb tests of tree frogs with different weights indicate the falling angles of species mostly lie in the range of 120°~180°, and the larger body of specie usually obtains a lower falling angle [38] (Fig. 2 a, b). Considering the tested force per unit area of the climbing toe pads, their recorded experimental data, however, reflect a fact that larger tree frogs possess more efficient climbing toe pads. The tree frogs also develop a special strategy of modulating body that spreading the limbs out sideways (and to a more limited extent, forwards or backwards as well) to maintain adhesion on overhanging substrates when the title angle increasing [39]. Such change of climbing posture decreases the angle of contact between pad and surface, conducting a synergistic effect between friction and adhesive forces that declines the tendency of peeling.

When the climbing happening on rough surfaces covered in fast-flowing water, the experimants of Endlein et al. [14] show that the torrent frogs have superior abilities than the tree frogs due to the large epidermal contact area (Fig. 2 c). Moreover, our group found the newts possesses the similar ability of wet climbing that escaping from the glass tank with vertical walls. The experimental investigations reveal the detaching angles of newts are mostly larger than 90°, particularly on the surface with little water in which case the detaching angle is up to 180° [40] (Fig. 2 d).

In general, the toe pads possess an inherent ability for wet climbing, in spite of the behind mechanisms being not fully understood. Earlier authors assumed the wet adhesion of toe pads comes of a glue function of the mucus [41], but this was not verified by later experimental studies [13,37]. Instead, a synergistic function of capillary forces (the dominant role), rate-dependent viscous forces (Stefan forces) is widely favored [18,19], see Table 1. The common model of capillary force used for quantifying the meniscus outside the sphere-plane is given by [42]

$$F = 4\pi\gamma cR(1 - \frac{D}{\sqrt{\frac{V}{\pi R} + D^2}}), c = \frac{\cos(\theta_1 + \beta) + \cos\theta_2}{2} \qquad (1)$$

where F is capillary force, γ is the surface tension of the liquid, R is the sphere radius, β is the filling angle describing the position of the liquid meniscus, θ_1 and θ_2 are the contact angles of the liquid to the sphere and the plane, and D is the gap width (see Table 1). The alternative model of the capillary force of meniscus inserted between two planes is given as follows [20,43]:
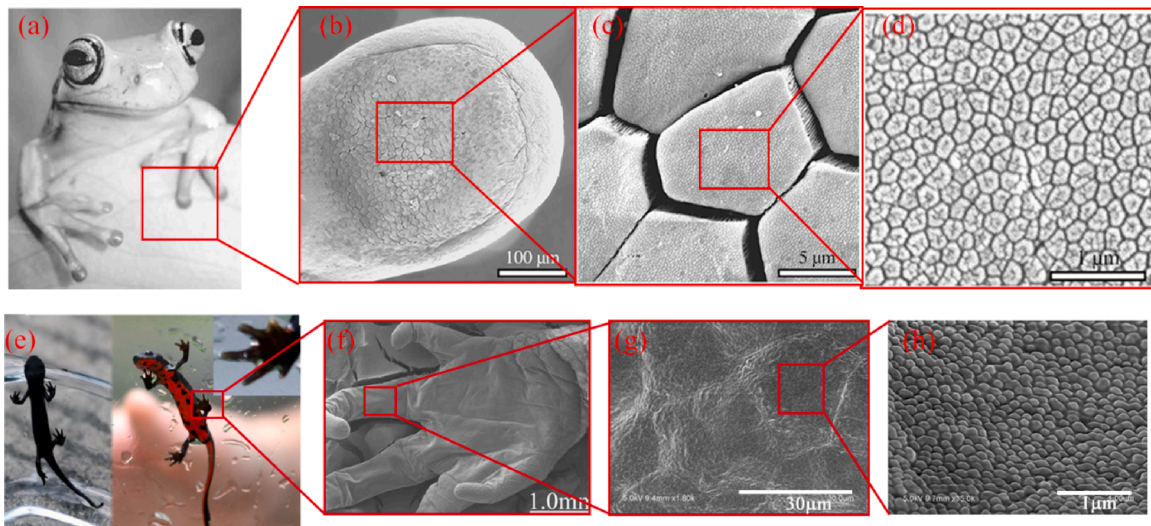

Fig. 1. (a) White's tree frog (Litoria caerulea); (c-d) morphology of (b) frog toe-pad, source: adapted from Federle et al. [17]; (e) the newt creeping on wet glass; (f) the scanning electron microscopy (SEM) of newt pad; (g-h) magnified image of pad epithelium including the polygonal cell and hemispheric bulges, source: adapted from Huang et al. [15].
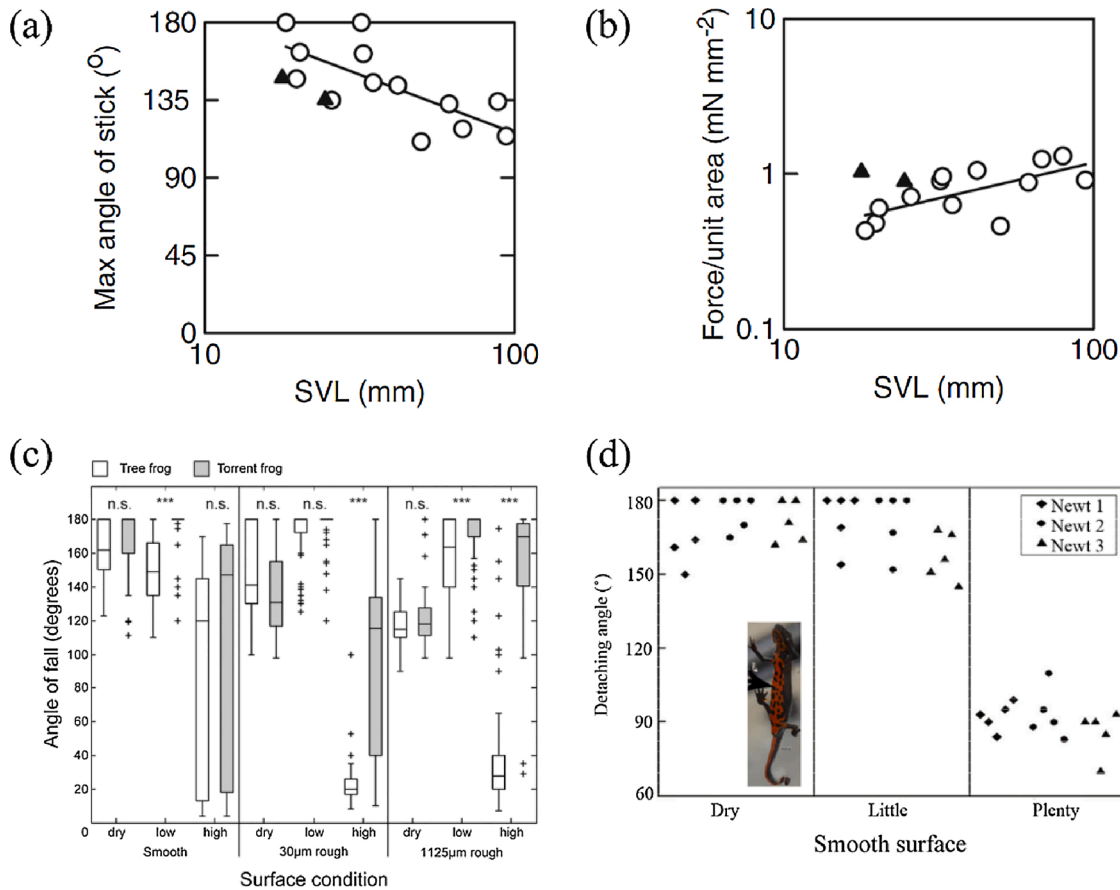
Fig. 2. (a) Falling angle and (b) adhesion force per square millimeter measured on 15 tree frogs, the snout vent length (SVL) reflecting the difference of body mass in tree frogs, source: adapted from Barnes et al. [38]; (c) fall angles between the tree frog and the torrent frog on different wet and rough surfaces, source: adapted from Endlein et al. [14]; (d) detaching angle of the newts on glass surfaces, source: adapted from Wang et al. [40].

Table 1
Typical force generation underlying wet attachments.

Force model	Schematics	Equations
Capillary force		(a) meniscus between sphere-plane $F = 4\pi\gamma cR(1 - \dfrac{D}{\sqrt{\dfrac{V}{\pi R} + D^2}}), c = \dfrac{\cos(\theta_1 + \beta) + \cos\theta_2}{2}$ (b) meniscus between flat-flat $F = \pi r^2 \gamma\left[r^{-1} - (\cos\theta_1 + \cos\theta_2)h^{-1}\right] - 2\pi r\gamma$
Viscous force		$F_V = -\dfrac{dh}{dt}\dfrac{3\pi\eta r^4}{2h^3}$
Friction force		$F_f = mg\sin(\alpha)$

$$F = \pi r^2 \gamma\left[r^{-1} - (\cos\theta_1 + \cos\theta_2)h^{-1}\right] - 2\pi r\gamma \qquad (2)$$

where r is the radius of meniscus, θ_1 and θ_2 are the contact angles of the liquid to the up and down plane respectively, h is the gap distance of two planes. When separating two rigid plates submersing in a fluid, the applied force will be resisted by a viscus obstruction of fluid flowing into the gap generating between two plates. This obstruction effect will be greater for more viscous fluids and for smaller distance of two rigid plates. The corresponding mathematic model is given by

$$F_V = -\frac{dh}{dt}\cdot\frac{3\pi\eta r^4}{2h^3} \qquad (3)$$

where η is the viscosity of liquid and t is the time for separating the two plates, h is the distance of two plates, r is the radius of plates.

Moreover, van der Waals forces can not be excluded because the direct contact may happen between the outer layer of toe pad and the substrate with the sandwiched fluid less than 35 nm [20]. Recent researches have suggested that the wet attachments of pads on inclined surfaces mainly arises from the interfacial frictions, where the epidermal structures, the secreted mucus and the material property of toe pads play an important role [16,17,24,44], see Table 1 for the mathematical model. In the following, we will focus on the physical principles underlying the interfacial behavior of toe pad wet contacts.

3. The microstructures for wet adhesion and friction

3.1. Toe pads' micro/nano structures and their function

The soft domed pads of above amphibians are usually characterized by additional surface features, which seem to contribute to their better capacity to attach to wet surfaces [14,15,18,19,40,45]. Appearing smooth at low magnification, the toe pads, in fact, evolved polygonal micro-structures of outermost layer separated by mucus-filled channels. The most striking is the regular hexagonal one, found in representatives of tree frogs; the diameter of single epidermal cell is approximately 10 μm surrounded by the about 1 μm wide channels (Fig. 1 a–d). In torrent frogs, the hexagonal epithelial cells have become elongated, with relatively straight channels running across the pad in a distal proximal
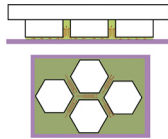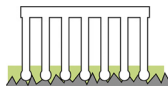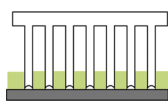
direction. The surface topography of newts's toe pads presents somewhat difference that the epidermis is characterized by irregular polygonal cells of approximately 30 μm in size, and the separated networking grooves are more shallow and narrow, of about 0.5 μm in wide (Fig. 1 e–h) [15,40]. These designs of regular or irregular polygonal array of channels surrounding each bulge epithelial cell were believed as function to spread the secreted mucus evenly over the pad surface and, under wet conditions, expel redundant fluid out, achieving a close contact with the substrate (calling draining effect) [16]. Moreover, the presence of grooves could facilitate attaching by contact splitting effect, reducing the crack propagation of pad peeling induced by body weight [20]. Pull-off stress would be spread between a larger number of hexagons rather than being concentrated at the edge of the contact zone.

At the nanoscale, the top of polygonal columnar cell is not smooth, but is featured by a dense array of nano patterns. For tree frogs, the nanopillars are of approximately 300–400 nm diameter, and 200–300 nm in height; the terminal tip is usually a concave shape (Fig. 3a–b, d–e) [21,46]. Although the true role of this nanostructure is not yet known, researchers speculate that they presumably give rise to a suction effect for attaching especially under wet conditions [46], where the reversible adhesion may be a result of the alternated pressure in chamber seal via the play of toe pad muscle [47,48]. Turning attention to the newts' toe pads, their polygonal cell surfaces contains countless hemispheric bulges of approximately 300 nm surrounded by smaller channels [15]. In the same way, the function of these nano pegs now still remain elusive, but the greater climbing ability of newts on the rough surface than the smooth one suggest that they may behave an interlocking effect under wet conditions (Fig. 3c, f) [40]. All in all, the functions of epidermal structures on toe pads for the wet attachments are summarized Table 2.

3.2. Hexagonal patterns for adhesion and friction

The draining effect of hexagonal arrangement of pad surfaces was considered to facilitate the wet attachments with various reasonable hypothesis [16], but it is difficult to give rigorous experimental evidence

Table 2
Functions of epidermal structures underlying wet attachments.

Function models	Schematics	Outlines
Draining effect		The array of hexagonal pillars expel redundant fluid out of the epidermis contacts [22], intimately contacting the substrates (close contact [16]) and preventing hydroplaning [25] (boundary friction [17])
Interlocking effect		i) For tree frog, Barnes' work suggest the interlocking may perform in pad friction [49] rather than wet adhesion force [19]. ii) For newts, our experiments indicate the interlocking of nano pegs presumably play a positive role for the wet attaching because of the higher falling angle on rough surface [40].
Suction effect		The nanopillars on the top of hexagonal patterns in tree frog appear conical in shape with a concave top [46]. It was suggested that these nanopillars could act as miniature suction discs, but this has yet to be demonstrated [43,46].

on biological surfaces. As a result, scientists shift their focus to the artificial mimics for the further study of underlying mechanisms, and copying the remarkable ability of toe pads. Earlier work of Varenberg and Gob indicated that the hexagonal patterns function as a friction-oriented feature during the interfacial sliding (Fig. 4 a, b) [25]. In the dry case, the patterns smooth the sliding, eliminating the stick-slip events usually happening on flat elastomer, whereas in the wet sliding, the ones allow the fluid to escape from the interface into the net of the adjacent interconnected channels, draining the contact zone for a higher friction force than flat control. Starting from the point that why were hexagons, Huang et al. experimentally evaluated the differences between round and hexagonal designs for friction, and point out that
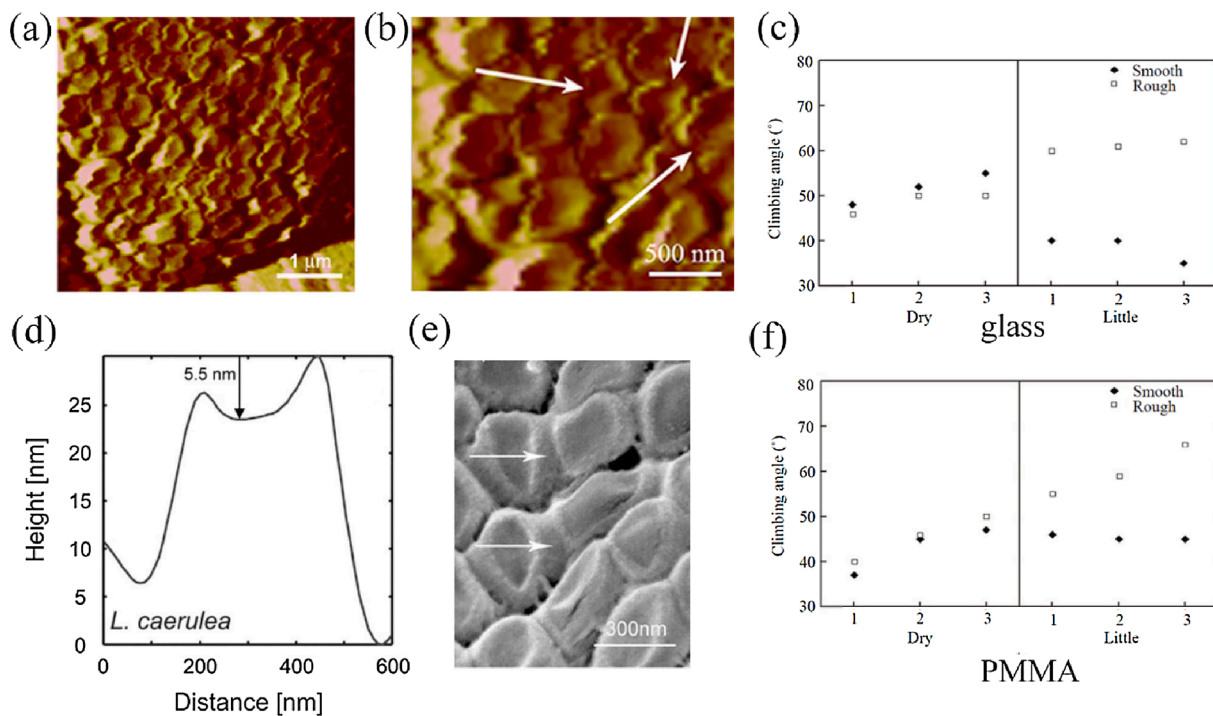

Fig. 3. (a-b) AFM images the detail appearance of the nanopillars (L. caerulea), source: adapted from Scholz et al. [21]; (c, f) climbing ability of the newts on glass and PMMA, source: adapted from Wang et al. [40]; (d) the topography of the dimples in nanopillars (L. caerulea), source: adapted from Barnes et al. [46]; (e) Cryo-SEM of the frozen nanopillars (R. prominanus), source: adapted from Barnes et al. [46].
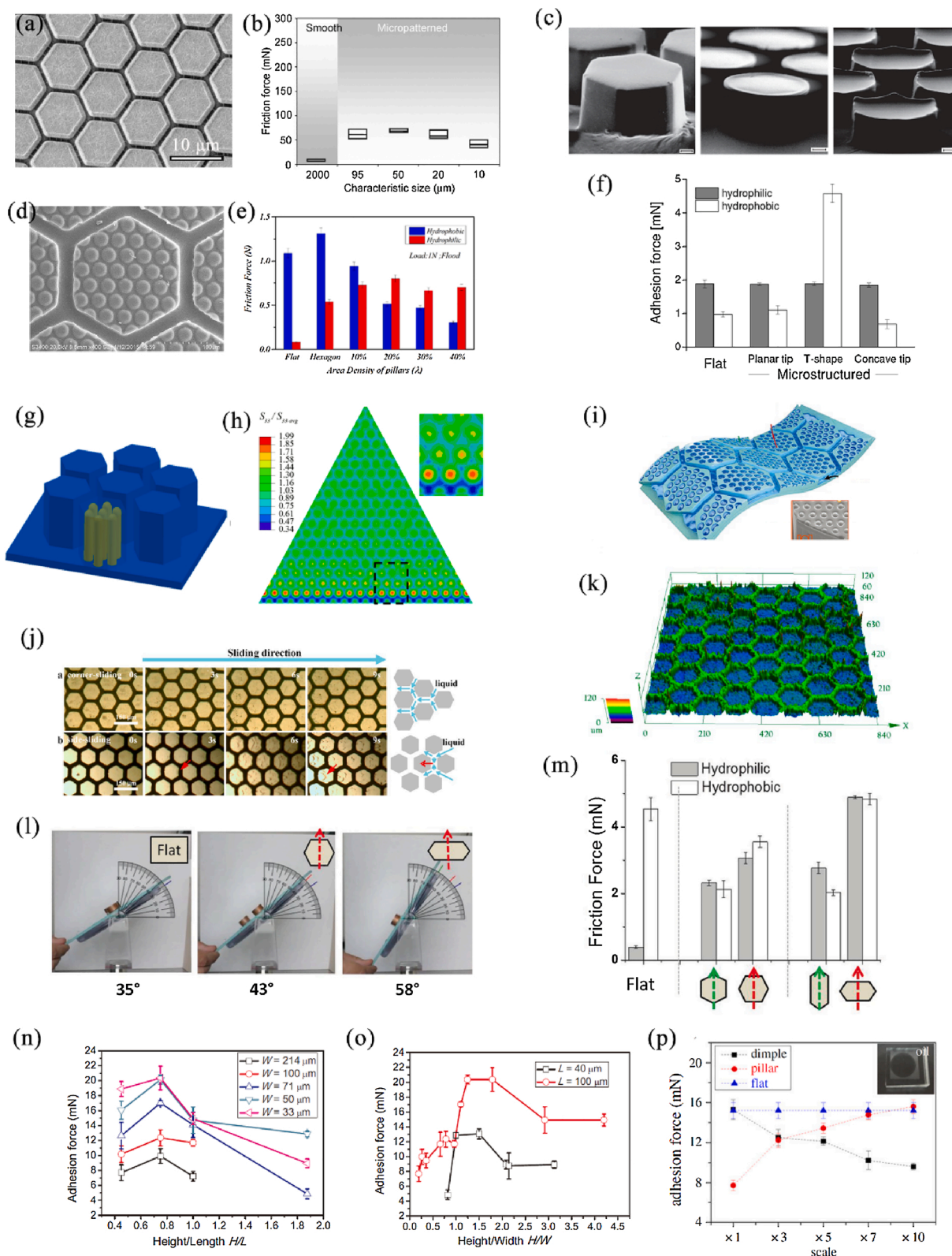
Fig. 4. (a-b) Frictional property of hexagonal pillars, source: adapted from Varenberg et al. [25]; (c) and (f) hexagonal pillars for wet adhesion, source: adapted from Drotlef et al. [16]; (d) and (e)adhesive property of hexagonal pillars; frictional property of peg-studded hexagonal patterns, source: adapted from Li et al. [51]; (g-h) nanopillars embedded in soft hexagonal micropillars and their stress distribution, source: adapted from Xue et al. [52]; (i) composite structure of suction cups and hexagonal pillars, source: adapted from Kim et al. [51]; (j, l, m) anisotropic friction of hexagonal pillars, source: adapted from Iturri et al. and Chen et al. [24,50]; (k) deformation of pig liver pressed by hexagonal pillars at the load of 10 N, source:adapted from Chen et al. [50]; (n, o) evolution of maximum wet adhesion force with height-to-length (H/L) and height-to-width (H/W) of channels, source: adapted from Xie et al. [55]; (p) adhesion force versus geometry scale of dimples and pillars for oil wetting condition, source: adapted from Li et al. [57].

hexagonal pillars can acquire higher pattern densities leading to a more efficient draining behavior and producing a higher energy dissipation of sliding over discontinuous channels [15]. Taking into account that the watery mucus spreads over toe pads, the investigation on artificial mimics should also involve the interfacial wetting factor. Drotlef et al. study the adhesion and friction behavior of plasma treated hexagonal pillars and untreated one, on which the lubricated fluid layer shows hydrophobic and hydrophilic respectively (Fig. 4 c, f) [16]. For adhesion under the hydrophobic regime, the direct contact forces dominate the interfacial behavior where the hexagonal patterns play a beneficial role following the rules of gecko-like adhesives, whereas in the hydrophilic regime, only the capillary forces contribute which exhibit little difference between patterned and unpatterned surfaces. However, the friction behaves conversely: in the hydrophobic case where the direct contact dominates, the hexagonal pillars lead to a lower friction then the flat control due to the loss of contact area; but for hydrophilic regime, the draining effect of hexagonal designs restrain the hydroplaning during sliding, resulting in a significantly higher friction forces. In nature, the direct contact force is a dewetting phenomenon, which will still come out under the mostly wetting case of $0° <$ contact angle $< 90°$ because of the spreading parameter $S < 0$ (it will be detailly discussed in section 3), but the repulsion of polar group induced by the oxygen treatment seems separate the contact pairs under the wet condition. To sum up, the polygonal array of epidermal cells evolved on toe pads appear to function more efficiently for friction than adhesion in wet attachments [44]. Moreover, compared with the tooth texture, the hexagonal patterns also have the ability of low deformation on the against surface under a same load, which is very suitable to decorated surgical grasper for the less tissue damage (Fig. 4 k) [50].

3.3. Composite patterns for adhesion and friction

Further focus on toe pads in nano scale, the top topography of the polygonal columnar epidermal cells exhibits countless finer structures, such as the nanopillars with concave terminal for tree frogs or the hemispheric bulgy cells, also referred to as "pegs," for newts. A few attempts have been conducted to comprehend the effect of such hybrid structures on the interfacial adhesion and friction. Our group reported the hexagonal micropillars with even smaller bulges on top surface fabricated by combining hemispheric crater arrays on wafer and conventional photolithography (Fig. 4 d, e). The array of top bulges qualify the ability of breaking the continuous lubricant film established in sliding contacts in hydrophilic case by the stress concentration to enhance the dewatering of hexagonal-channels, presenting a higher friction than hexagonal patterned and flat surfaces [51]. Xue et al. fabricated the array of hexagonal micropillars with embedding aligned relative hard nanopillars (Fig. 4 g, h) [52]. Compared with the pure pillars, both adhesion and friction forces of composite structure were greatly improved. The mechanisms were suggested that the embedded nanopillars shift the stress maximum from the edge of contact interface to top area of a row of nanopillars close to the micropillar perimeter, restraining the crack withdrawing for detaching. Kim et al. decorated the head of hexagonal micro pillars by octopus-like convex cups (Fig. 4 i): this 3D architecture combines the arresting effect against crack propagation of microchannel network and the suction effect of cups achieving a prominent adhesion on skin in sweaty and even flowing water conditions [53].

3.4. Orientation of hexagonal patterns for frictions

It has been suggested that the hexagonal patterns against hydroplaning play a very important role for wet attachments. The anisotropy design of pattern geometry along the shear direction, however, will certainly shows orientation dependence for friction. Chen et al. reported that the regular hexagonal pillars exhibit more friction in the corner direction than the side one, and the smaller of corner angle is the

stronger difference perform [50]. Visible views of sliding show that the liquid in corner sliding flowed smoothly to the hexagon angle and then split into two-way flowing through the tilt channels, but in side sliding, the liquid converged in channels adjacent to sliding side of patterns, and could be squeezed out, flushing into the contacts of sliding (Fig. 4 j), which are probably responsible for that friction difference. However, Iturri et al. hold different views that the hexagonal pillars showed higher friction along the direction of side sliding after considering the hydrophilic case and the pillar height (Fig. 4 l, m); the elongated pillars got even higher than the regular ones [24]. Both the low bending stiffness of the pillars for effective liquid drainage and the high edge density per unit length of patterns for effective arresting of cracks in the sliding direction are the key factors for that enhanced friction. These suggestions were further confirmed by the micro friction maps of AFM probe sliding and the macroscopic experiment of the angles of patterned surface sliding on tilting stages flooded with water [24].

3.5. The aspect ratio, size scale and concave-convex shape for polygonal patterns' performance

The height, radius, aspect ratio, size scale, etc., of micropillars have been demonstrated deeply influencing their dry adhesion performance [54]. Analogically, the geometrical parameters of hexagonal patterns may also play an important role for the wet adhesion, which need to be optimized when designing for practical application. Research shows that single factors alone, such as the width (W), length (L), and height (H) have a slight effect on the wet adhesion force, whereas the values of width to length (W/L), height-to-length (H/L), and height-to-width (H/W) of channels determine significantly [55]. The wet adhesion force is reduced with increasing W/L values owing to the reduction in the actual contact area between the two flat surfaces. Optimal ranges of H/L and H/W values clearly enhance the wet adhesion force, even considering the reduction with the increasing W/L values, by the deformation of pillar and the drainage capacity of channels (Fig. 4n, o). As presented in 3.1 section, the toe pads of tree frogs show hexagonal patterns in micro scale which are "open" to liquids, but in nano scale, the evolved concave shape tip of nanopillars are "close" to liquids. Such an inverse orientation of structures is interesting when evaluating and comparing their interfacial behaviors under a same condition with the consideration of scale effect [56]. Our results shown that polygonal pillars significantly enhanced the surface wettability depending on size scale, whereas the micro dimples suppressed the wettability with independence of size scale (Fig. 4p). Polygonal pillars improved the surface wet adhesion force with increasing size scale, but the micro-dimples performed inversely.

4. The role of wedged film and bulk softness for contacts and adhesions

4.1. Soft bulk

4.1.1. The physical properties of biological toe-pads (the structures underlying surface and the elastic modulus)

Present studies of anatomy showed the epithelium of toe pads of amphibians, such as the tree frog and torrent frog, were stratified, consisting of at least four layers (Fig. 5a–c) [45,46]. The outermost layer is keratinised and nonliving with a much larger thickness (about 15 μm for tree frog), which may have a function of resisting the injury and the abrasion during attaching on rough surfaces. This layer is stained darkly, whose outer region is separated by the interlinked channels [21]. The structure of second layer cells resembles remarkably the outer layer, with a result of growing the outer layer through the shedding of the outer layer. In addition, the underlying dermal tissue between the terminal phalanx and the ventral epidermis is highly vascularised, which might allow an active modification of pad curvature and pad stiffness by varying blood pressure [58]. Without any contacts, the surfaces of toe
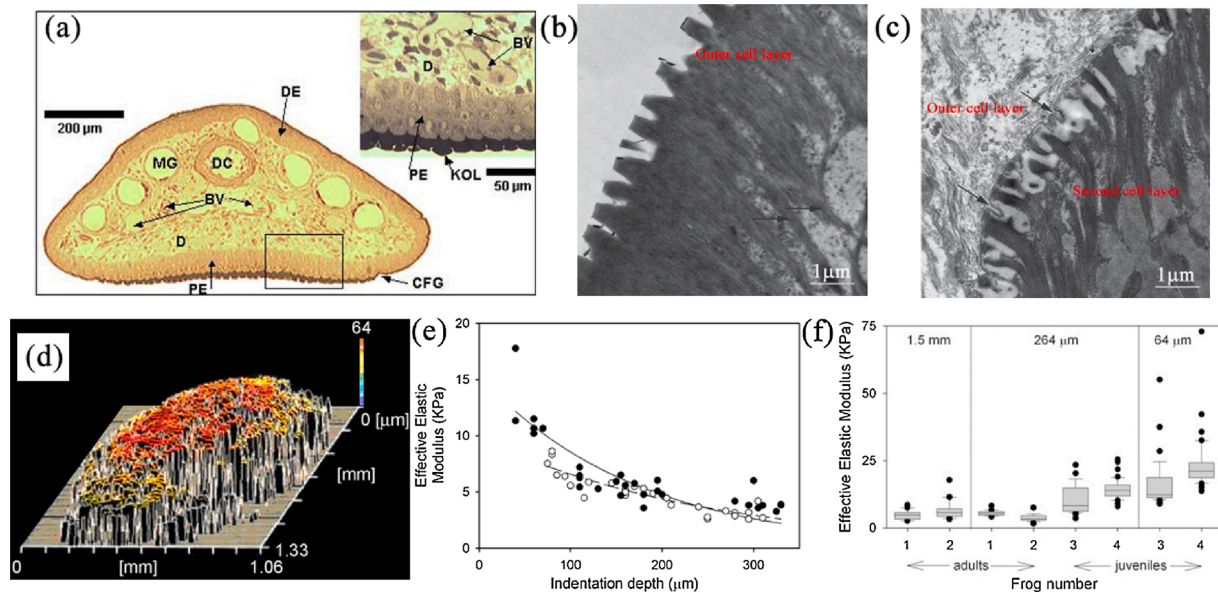
Fig. 5. (a) Transverse section of toe of immature *L. caerulea* stained with toluidine blue to show its internal anatomy, source: adapted from Barnes et al. [23]; (b, c) structure of outer cell layer and its transition boundary transmission of toe pad epithelium in the electron microscopy (TEM) images of *S. parvus digits*, source: adapted from Drotlef et al. [45]; (d) a 3D reconstruction of toe pad shape (*oblique plot*), source: adapted from Barnes et al. [23]; (e, d) effects of indentation depth, indenter diameter (1.5 mm, 264 and 64 μm) and frog age on effective elastic modulus, source: adapted from Barnes et al. [23].

pads naturally show domed outline (Fig. 5d) [23], and the nano indentation tests of atomic force microscope display that the effective elastic modulus of the outer keratinized layer lie in 5−15 MPa [21]. That stiffness is equivalent to silicone rubber, but an intuitive insight is that the overall bulk is extremely soft, which can give a high compliance to any rough surfaces. Micro-indentation studies have been performed, and quantitatively reported that the whole toe pads of the tree frog (Litoria caerulea) with a deep deformation inside has an effective elastic modulus of 4–25 kPa (Fig. 5e, f) [23]. Moreover, the features of force-depth curves also provided some other evident characters of toe pads: the gradient stiffness in the section, the viscoelasticity, the elasticity rather than plasticity. With such physical properties, the toe pads were proposed to allow a degree of modulating of contacts to substrates, such as the intimate contact with surface profiles or the contact hysteresis, which improves both the interfacial friction and adhesion.

4.1.2. Softness for the indentations, detachments and draining effect

The superiority of the softness in the toe pads for wet attachments still lay in reasonably assumption, where the experimental evidence for illustrating the underlying mechanisms was desired. We carried out a study on the indentation and detachment on a very soft silicone, mimicking the toe pad bulk (elastic modulus of about 0.6 MPa, shore hardness of about 35), in comparison to the JKR theory (pure elastic material) [59]. It is shown that the deformation of soft material usually accompanied with a viscoelastic loss undergoes a hysteresis of bulk elastic response leading to an energy dissipation in the contact system (Fig. 6a). In the indentation by loading, the viscoelastic dissipation reduces the stored elastic energy of bulk that allows the correlation of load-penetration to present a roughly linear transformation from JKR mode to Hertz mode; but it seems to have little effect on the stored interfacial energy with the input of external work, which was reflected by the result that the relation between force and contact radius is always close to the JKR expectation (Fig. 6b, c). The viscoelastic dissipation also functions the detachment of the probe retraction, which is characterized with a pronounced stick-split phenomenon. The first one is stick region where the soft material firmly sticks the probe without contact area decreasing, behaving as flat punch detachments, and then the split region starts giving the highest pull-off force, which is far exceed the JKR prediction (Fig. 6d, e). Actually, the crack motion of contact edge in the

detachment follows the crack propagation principle of Griffith's criterion. The stick region is configured with G (energy release rate) $\leq \Delta\gamma$ (work of adhesion). When the mechanical energy dissipated by viscoelastic losses is insufficient to break through the barrier of surface energy stored in the crack tip of the contact edge, it can be described as

$$\begin{cases} U_E + U_F - U_{diss} \leq U_S \\ G = G_M(F, \delta) - G_{diss} \leq \Delta\gamma \end{cases} \tag{4}$$

where G_M is the original strain energy release rate and G_{diss} is the energy dissipation term. G_{diss} is attributed to the slight stress relaxation and the creep in dwell time of the contact and the viscoelastic loss in detachment. The increase in G_M in the initial probe retraction mainly offsets G_{diss} with a fixed contact area until the case of $G = \Delta\gamma$, where the crack of the contact opens, and then the split region begins though the dissipative item of G_{diss} still behaving, and a much higher pull-off force will be achieved.

The above summarize the general physical behaviors of the indentation and detachment on soft viscoelastic materials. When introducing the hexagonal pillars to wet contacts, the softness factor of material also plays a beneficial role for the performance of the structures for adhesion. Experimental results demonstrated that the pull-off force of adhesion in a totally wetting case increased along with the increase of surface softness [60]. Insights into the force-displacement curves, the softness seems to improve the short-range contribution caused by the "close contact", but show little effect on the long-range contribution of capillary force. Based on the suggestions in previous sections, the array of hexagonal pillars have effects on draining liquid and increasing contact compliance throughout the interface. As a result, the softness is likely to enhance the drainage effects and the contact compliance of hexagonal pillars, which produced a closer and larger area of contacts in wet adhesion, resulting in a stronger adhesion force (Fig. 6g, h). In addition, the energy dissipation of viscoelasticity functioning in soft pillars also promotes the adhesion forces. Rao et al. have further employed the breaking of dynamic ionic bonds in tough hydrogels to amplify the energy dissipation hexagonal pillars for increasing the adhesion strength underwater (Fig. 6f) [61].
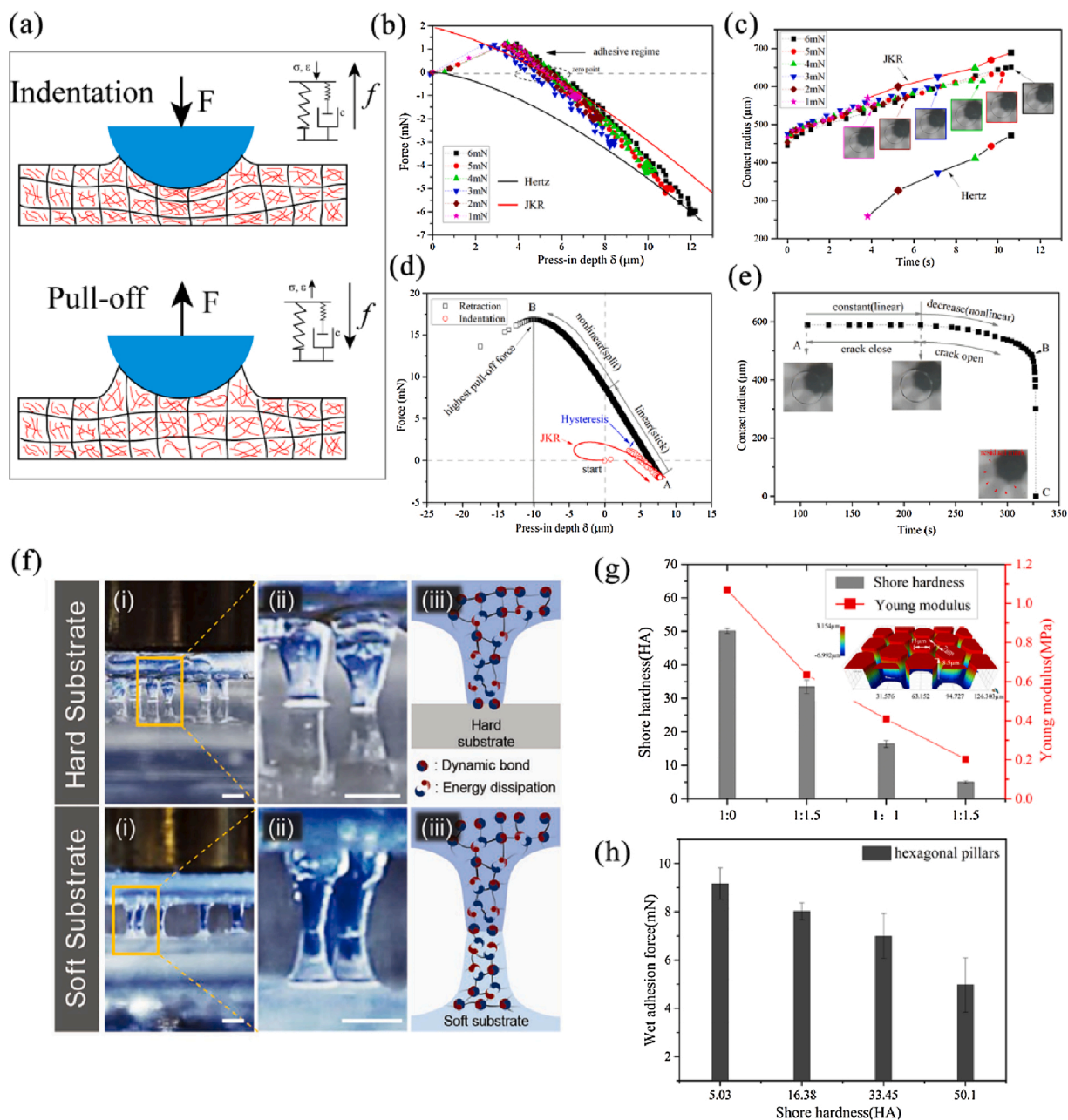
Fig. 6. Indentation and pull-off behavior on viscoelastic materials: (a) schematic of deformation of soft surface, (b) load force and (c) contact radius in indentation, (d) pull-off force and (e) contact radius in detachment, source: adapted from Li et al. [59]; (f) energy dissipation in debonding of hexagonal pillars to the hard and soft surface, source: adapted from Rao et al. [61]; (g-h) effect of softness on the wet adhesion of hexagonal pillar patterned surface, source: adapted from Li et al. [60].

4.2. Thin film

4.2.1. The thickness on toe pads and the wedged film instability for direct contacts

Numerous glands within the amphibious toe pads ceaselessly secrete watery mucus that wets the whole epidermal surfaces through narrow ducts which open into the grooves [62]. When toe pads contact against the substrates, the mucus wedged between the contact regions and forms a liquid bridge with a meniscus around the edge of the pad [13,38]. The viscosity of mucus (tree frog) is reported with the value of about 1.5 MPa s by a technique of laser tweezer, that is, 1.5 times the viscosity of water [17]. Whether or not the mucus belongs to Newtonian liquid remains controversy so far [20,58], still needing a further study. The mucus, however, has been suggested to contain molecules that act as surfactants lowering the surface tension. The mucus on both hydrophilic and

hydrophobic surfaces can present a very low static contact angle value ($\leq 10°$), meaning that the pad capillary force is independent of the surface energy of the substrate [16]. Using the interference reflection microscopy, Federle et al. have shown that the mucus layer between the contact of the toe pad (tree frog) and glass have a lower thickness [17]. Most of the toe pad epithelial cells presented dark regions, reflecting the nanoscale film thickness (ranges from 0 to 35 nm, Fig. 7a–d). Considering the fluid inserted in narrow channels of the array of nanopillars, the tops of many nanopillars in the attaching of toe pads were proposed to be in a direct contact with the substrate. To sum up, the characteristics of wedged fluid film influence the contact mode between the toe pad and the substrate, which determining the mode of action in wet adhesion, such as direct contact force, capillary force, etc.

In fact, the wet contacts between the toe pads and the substrates can be simply regarded as the soft rubber contacting a solid surface under
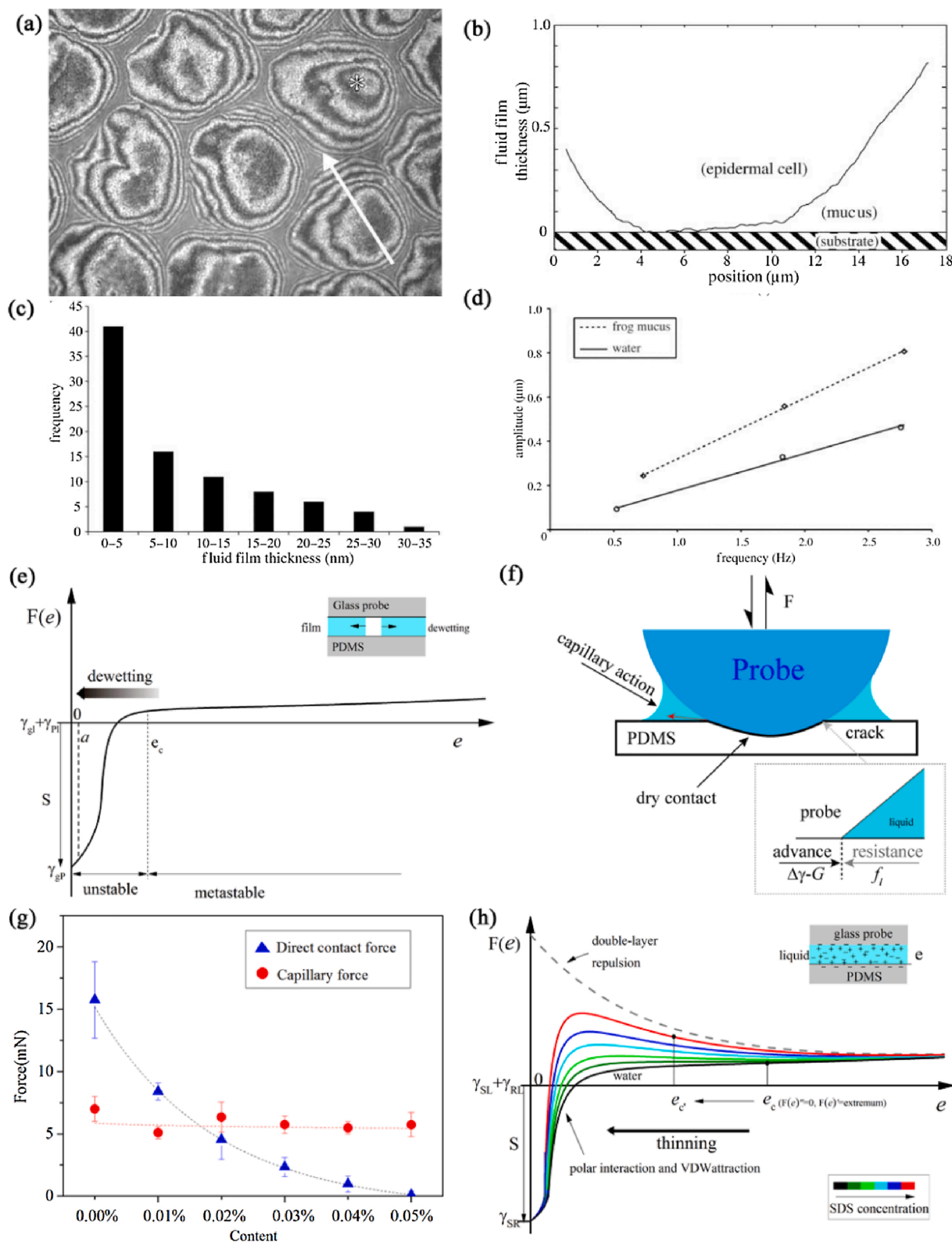
Fig. 7. Property of thin film of mucus between tree frog toe pad and substrate: (a) the interference images of pad contact with glass, (b) the thickness of fluid film along the white arrow in (a), (c) frequency of fluid thicknesses measured between hexagonal patterns and glass, (d) relationship of bead displacement amplitude and velocity (frequency) measured for toe pad mucus and pure water (the slopes reflect the fluid viscous), source: adapted from Federle et al. [17]. Mechanisms behind the dewetting behavior of wedged film in wet adhesion: (e) free energy of wedged water film between glass and rubber, (f) schematic of the effect of wedged fluid on the contact between the probe and soft PDMS, (g) the direct contact and capillary force contribution in wet adhesion with varying SDS solution, (h) influence of electrical double-layer repulsion on the free energy of wedged film, source: adapted from Li et al. [59,63].

wet conditions, where the wedged film behavior depends on the sign of the spreading parameter S, which can be expressed as

$$S = \gamma_{SR} - (\gamma_{SL} + \gamma_{LR}) \tag{5}$$

where γ_{ij} are the solid/rubber, solid/liquid, and liquid/rubber interfacial tensions. It compares interfacial energies between 'dry' contacts γ_{SR} and lubricated contacts $\gamma_{SL} + \gamma_{RL}$ of liquid/solid interface [64–66]. If S is positive, the wedged film is stable and performs as an interlayer in contacts, and the capillary forces generally dominate the adhesive strength. The exception, however, is that when the interacted film is thin enough that the close contact induced by van der Waals may also contribute for adhesion, e.g., the case of tree frog pad contacts or the contact of rubber and glass under silicone oil. When S is negative, the wedged film between wet contacts is unstable, and easily collapses for direct contacts, called the dewetting phenomenon, under thinning by a preload; in comparison to capillary forces, the direct contact forces usually play the dominant role in wet adhesion. The transformation of the wedged film from stable to unstable in dewetting phenomenon depends on the film thickness in wet contacts. The free energy F of wedged film versus its thickness e is given by [65,67–72]

$$F(e) = \gamma_{SL} + \gamma_{RL} - \frac{A}{12\pi e^2} - 2\gamma_L^P \exp[(a-e)\big/l] + \frac{1}{2}\rho g e^2 \tag{6}$$

where γ_L^P is short-range polar contribution, ρ is liquid density, g is acceleration of gravity. A is the effective Hamaker constant which can be expressed by $A = A_L + A_{SR} - A_{RL} - A_{SL}$, a is the size of a liquid molecular, l is a correlation length for the polar fluid. For water, l appears to be in the range of 0.2 and 1 nm, and an estimate of the best value is about 0.6 nm [65]. Fig. 7 e qualitatively describe the free energy of wedged water $F(e)$ depending on e based on properties of formula components ($S < 0$). Briefly, $F(e)$ decreases with the film thickness e decreasing; and the critical value e_c ($\ll 1$ μm) is located at the second derivative $F''(e) = 0$. For mesoscopic films ($e > e_c$), the curvature of $F(e)$ is positive ($F''(e) > 0$), the film is metastable and the dewetting for direct contact requires a nucleation of a single contact point, but it is not easy to realize in the wedged case [73]. For nanoscopic films ($e < e_c$), the curvature of $F(e)$ is negative ($F''(e) < 0$), the wedged film is unstable and dewets spontaneously. When a wedged film thin to reaching e_c under loading, it will spontaneously collapse for the direct contact, and the contact area and the direct contact strength in wet adhesion rely on liquid surface tension and its contact angle on solids. The work of adhesion for direct contacts $\Delta\gamma_l$ in wet adhesion is [74]:

$$\Delta\gamma_l = \Delta\gamma - \gamma_l(\cos\theta_1 + \cos\theta_2) = -S \tag{7}$$

where $\Delta\gamma$ is the work of adhesion for the dry contact in air, γ_l is the surface tension of liquid, θ_1 and θ_2 are the contact angles of liquid on two solid surfaces respectively. As the same to dry case, the contact edge between two solids in liquid advances as the crack recedes. The driving force for this advance for increasing contact area can be thereby given as:

$$\Delta\gamma_l - G = \Delta\gamma - G - \gamma_l(\cos\theta_1 + \cos\theta_2) = \Delta\gamma - G - f_l \tag{8}$$

Here $f_l = \gamma_l(\cos\theta_1 + \cos\theta_2)$ is the effect of liquid on the movement of the crack of contact edge. Compared with the dry case of $\Delta\gamma - G$, the liquid will perform a resistance for the advance of contact edge if $\cos\theta_1 + \cos\theta_2 > 0$, but the capillary action of liquid surrounding the contact area mostly provides an drive force on the contact edge (see the schematic in Fig. 7f) [74–76].

In addition, we have found the direct contact force in wet adhesion can be tuned by the supplement of double-layer force. Fig. 7 g shows direct contact force of water adhesion between PDMS and glass decreases with the increased content of sodium dodecyl sulfate (SDS), and at a high concentration of SDS solution, the direct contact force vanishes, leaving only capillary force contributing the wet adhesion. When

adding the SDS to water, the free energy mode of wedged film can be modified as [77–80]:

$$F(e) = \gamma_{SL} + \gamma_{RL} - \frac{A}{12\pi e^2} - 2\gamma_L^P \exp[(a-e)\big/l] + \frac{1}{2}\rho g e^2 + \frac{k}{2\pi}Z\exp(-ke) \tag{9}$$

where k^{-1} is the Debye length, Z is a interaction constant, which is analogous to the Hamaker Constant A (details see ref. [81]). Though the interfacial energies of $\gamma_{SL} + \gamma_{RL}$ and γ_L^P change with the addition of SDS molecules, our study demonstrated that it is the potential energy induced by electrical repulsion that imposes the free energy curve with a concave shape (similar to DLVO theory [82]), see Fig. 7 h, weakening the collapse of wedged film and eliminating the direct contact force for the wet detachment.

5. Strategies of switchable capillary forces

5.1. Some ways to adjust the capillary adhesions

Turning focus back to the toe pads, the physical mechanism of wet adhesion to a variety of surfaces is quite complicated, but capillary forces and viscous forces generally accepted as the two main contributions for the normal adhesives. After examining the relationship between toe pad area and adhesive force in different tree frog species (Fig. 8a), Barnes suggested that the capillary force is the main component of wet adhesion rather than the viscosity one [19]. In nature, the amphibians seem to have evolved an advanced ability of dynamically regulating capillary interaction for the switchable adhesives on wet substrates. To explain the background mechanisms, some hypotheses such as the dynamic actuation of the epidermis's topography or modulating the amount of liquid meniscus, have been proposed [22,83]. The possibility of the chemical modification of the epidermis's secretion to turn capillary interactions for reversible adhesion cannot be excluded [16].

From the view of basic physics and chemistry, the capillary force of meniscus inserted two substrates is dominated by the interfacial property of solid/liquid suffering from the influence of solid geometries [42, 84,85], environmental conditions [86–88], materials [89,90], etc. Some approaches, such as changing material shape [91–93], splitting wedged film [94], modifying surface chemicals [95,96], or employing contact-angle hysteresis [97–99], have been developed experimentally or theoretically (Fig. 8b–d). However, these alterations of capillary effect seem cumbersome, permanent and irreversible, and difficultly to achieve a timely response of capillary switching *in situ*, allowing a large gap to capillary on biological epidermises of amphibian toe pads.

5.2. Magnetically stimulating for switchable capillary forces

Fascinating examples were developed in mimicking reversible regimes of hairy dry adhesion of geckos, which mainly utilizing surface topography reorganization via the application of an external physical stimulus, such as temperature [100–102], magnet [103,104], or preload [32–34], providing new ideas of intelligently regulating the capillary adhesion artificially. Recently, we develop a reversible adhesion system that two solid surfaces were filled by a magnetic fluid (MF) meniscus joint where the capillary effect undergoes alteration when smartly applying external magnetic stimuli [105]. In comparison to the original capillary force (without stimuli), the stimulated one increases or decreases depending on the distributions of applied magnetic field intensities, showing switchable behaviors (Fig. 8e). The original capillary force of MF meniscus is a main result of the pressure difference of liquid/air boundary between inside and outside, i.e., Laplace pressure (the pressure inside the meniscus is uniform). When the non-uniform magnetic field applies to the MF meniscus, the intensity difference will evoke a hydrostatic pressure [106–108] between the inner and outer surfaces
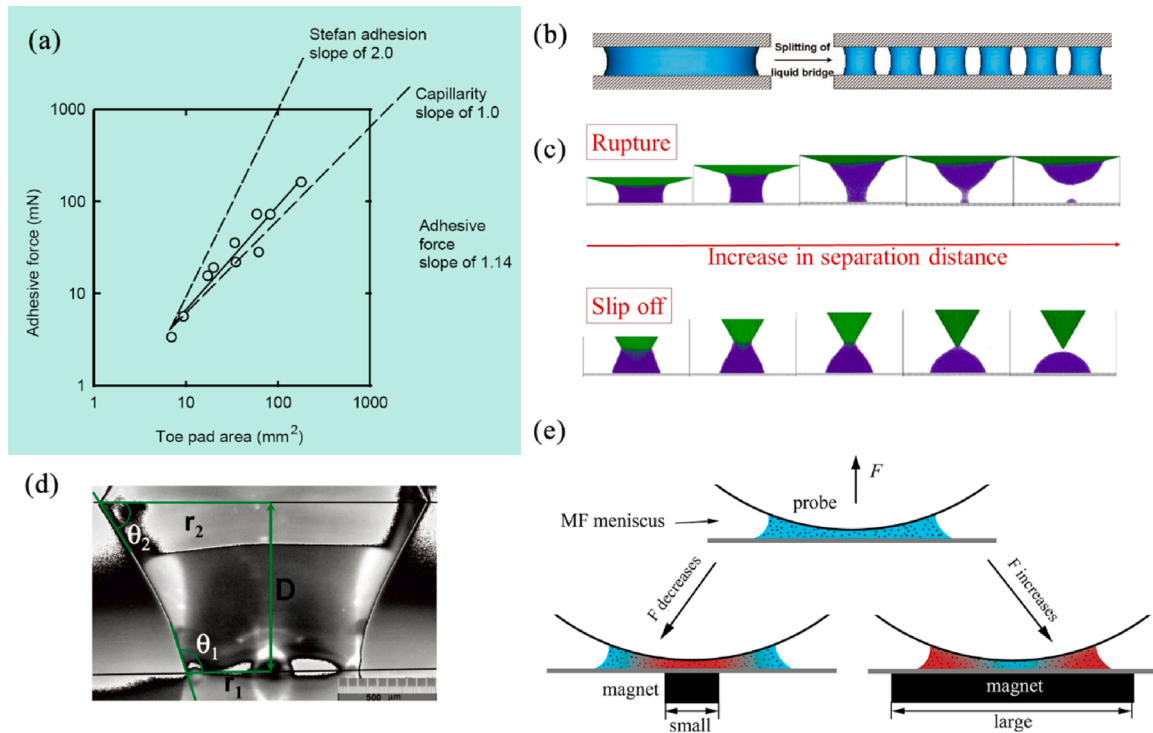
Fig. 8. (a) Relationship of adhesive force to toe pad area for tree frogs, source: adapted from Barnes [19]; (b) schematic of splitting effect on liquid bridge for enhancing the capillary force, source: adapted from Souza et al. [94]; (c) the rupture of liquid bridge inserted between a sphere/cone and a plane, source: adapted from Liang et al. [91]; (d) liquid bridge between chemically different substrates, source: adapted from Souza et al. [95]; (e) magnetically stimuli the liquid bridge for reversible capillary forces, source: adapted from Li et al. [105].

of the meniscus which imposes a tuning effect on the pressure inside the MF meniscus (such additional pressure distributes nonuniformly inside the meniscus), switching the adhesion strength. The physical model of MF meniscus (probe-MF-flat) can be given as

$$F_{capillary} = -4\pi\gamma R \frac{\cos(\theta_1 + \beta) + \cos\theta_2}{2} + \sum_{k=1}^{N}\left[\mu_0 M_s(H_i(k) - H_j(k))\right.$$
$$\left. - \frac{1}{2}M_n(k)^2\right]\frac{2k\pi L^2}{N^2}$$

Where $F_{capillary}$ is the capillary force, γ is the surface tension of the MF, R is the curve radius of probe, β is the filling angle, θ_1 and θ_2 are the contact angles of MF on the probe and substrate, μ_0 is the magnetic permeability of free space, M_s the saturation magnetization of MF, $H_i(k)$ and $H_j(k)$ are the field intensity along the probe surface and the meniscus surface respectively, $M_n(k)$ is the normal component of magnetization at the meniscus surface, L is the radius of MF meniscus.

To summarize, for weakening capillary adhesion of the MF meniscus, someone needs to increase positive magnetic field intensity difference between the inside and the outside of the meniscus; on the contrary, the desire of enhancing capillary force is to impose an inverse application on the meniscus. The above novel strategy of manual regulation for reversible capillary forces can be regarded as a guide for further study in developing new controllable wet-adhesive systems.

6. Conclusions and outlook

The toe pad wet adhesion and its biomimics have drawn much attention, and reached a high level of understanding over the last 10 years. The outstanding wet adhesion properties is primarily raised from the special designs of epidermis structures by which the capillary force, the friction force can be controlled and amplified on a wet substrate. Research work so far, though, have well revealed and confirmed some mechanisms behind the wet attachments, e.g., the draining effect of

hexagonal patterns, the boundary friction of close contacts, the visco-elastic dissipation of soft tissue, there are still many unknowns waiting to be explored, such as the following. i) Compared with the deep insight into the micro array of hexagonal patterns, the nature role of the nanostructures on toe pads in wet adhesion remains in reasonable speculation, starving for a better understanding from bioresearch and biomimicking. ii) Capillary forces and time-dependent viscous forces are considered as two main contributions for wet adhesion, but the functions of epidermis structures on them are not fully clear, much less the corresponding mechanism of the transformation on these forces between attachment and detachment. iii) What are chemical components of the toe pads' secretion? How does the interfacial character of the interaction in the secretion/ epidermis or the secretion/substrate contribute the wet adhesion including the friction force, the capillary force and the viscus force?

Moreover, the bioinspired strategy for artificial adhesive surfaces still face some challenges despite the wide applications. For instance, more advanced technologies should be developed for fabricating the complicated artificial adhesive structures (composite array of micro- and nanostrustures), synthesizing biocompatible material and applying the stimuli for the switching of interfacial behaviors. It is expected that as more secrets of toe pad wet adhesion and barriers of bionic technologies are unraveled, many novel solutions from bio-inspiration will be provided for artificial adhesive surfaces in many fields, such as intelligent robots, wearable devices (e.g., wet climbing, electronic devices), biomedicine (e.g., wound dressing and drug delivery), etc.

Declaration of Competing Interest

None.

References

[1] K. Autumn, Y.A. Liang, S.T. Hsieh, W. Zesch, W.P. Chan, T.W. Kenny, R. Fearing, R.J. Full, Adhesive force of a single gecko foot-hair, Nature 405 (6787) (2000) 681–685.

[2] K. Autumn, A.M. Peattie, Mechanisms of adhesion in geckos, Integr. Comp. Biol. 42 (6) (2002) 1081–1090.

[3] M. Scherge, S.S. Gorb, Biological Micro- and Nanotribology, Springer, Berlin, 2001.

[4] K. Autumn, Gecko adhesion: structure, function, and applications, MRS Bull. 32 (06) (2007) 473–478.

[5] K. Autumn, A. Dittmore, D. Santos, M. Spenko, M. Cutkosky, Frictional adhesion: a new angle on gecko attachment, J. Exp. Biol. 209 (Pt 18) (2006) 3569–3579.

[6] Y. Tian, N. Pesika, H. Zeng, K. Rosenberg, B. Zhao, P. McGuiggan, K. Autumn, J. Israelachvili, Adhesion and friction in gecko toe attachment and detachment, Proc. Natl. Acad. Sci. U. S. A. 103 (51) (2006) 19320–19325.

[7] A. Geim, S. Dubonos, I. Grigorieva, K. Novoselov, A. Zhukov, S.Y. Shapoval, Microfabricated adhesive mimicking gecko foot-hair, Nat. Mater. 2 (7) (2003) 461–463.

[8] L.F. Boesel, C. Greiner, E. Arzt, A. del Campo, Gecko-inspired surfaces: a path to strong and reversible dry adhesives, Adv Mater 22 (19) (2010) 2125–2137.

[9] M. Kamperman, E. Kroner, A. del Campo, R.M. McMeeking, E. Arzt, Functional adhesive surfaces with "Gecko" effect: the concept of contact splitting, Adv. Eng. Mater. 12 (5) (2010) 335–348.

[10] Y. Li, J. Krahn, C. Menon, Bioinspired dry adhesive materials and their application in robotics: a review, J. Bionic Eng. 13 (2) (2016) 181–199.

[11] R. Hensel, K. Moh, E. Arzt, Engineering micropatterned dry adhesives: from contact theory to handling applications, Adv. Funct. Mater. (2018) 1800865.

[12] D.M. Green, Treefrog toe pads: comparative surface morphology using scanning electron microscopy, Can. J. Zool. 57 (10) (1979) 2033–2046.

[13] S.B. Emerson, D. Diehl, Toe pad morphology and mechanisms of sticking in frogs, Biol. J. Linn. Soc. 13 (3) (1980) 199–216.

[14] T. Endlein, W.J.P. Barnes, D.S. Samuel, N.A. Crawford, A.B. Biaw, U. Grafe, Sticking under wet conditions: the remarkable attachment abilities of the torrent frog, Staurois guttatus, PLoS One 8 (9) (2013) e73810.

[15] W. Huang, X.L. Wang, Biomimetic design of elastomer surface pattern for friction control under wet conditions, Bioinspir. Biomim. 8 (4) (2013) 046001.

[16] D.M. Drotlef, L. Stepien, M. Kappl, W.J.P. Barnes, H.J. Butt, A. del Campo, Insights into the adhesive mechanisms of tree frogs using artificial mimics, Adv. Funct. Mater. 23 (9) (2013) 1137–1146.

[17] W. Federle, W.J. Barnes, W. Baumgartner, P. Drechsler, J.M. Smith, Wet but not slippery: boundary friction in tree frog adhesive toe pads, J. R. Soc. Interface 3 (10) (2006) 689–697.

[18] W.J.P. Barnes, J. Smith, C. Oines, R. Mundl, Bionics and wet grip, Tire Technol. Int. 2002 (December) (2002) 56–60.

[19] W.J.P. Barnes, Tree frogs and tire technology, Tire Technol. Int. 99 (0) (1999) 42–47.

[20] W.J.P. Barnes, Adhesion in Wet Environments: Frogs, Springer, Netherlands, 2012.

[21] I. Scholz, W.J. Barnes, J.M. Smith, W. Baumgartner, Ultrastructure and physical properties of an adhesive surface, the toe pad epithelium of the tree frog, Litoria caerulea White, J. Exp. Biol. 212 (Pt 2) (2009) 155–162.

[22] B.N.J. Persson, Wet adhesion with application to tree frog adhesive toe pads and tires, J. Phys. Condens. Matter 19 (37) (2007) 376110.

[23] W.J.P. Barnes, P.J.P. Goodwyn, M. Nokhbatolfoghahai, S.N. Gorb, Elastic modulus of tree frog adhesive toe pads, J. Comp. Physiol. A 197 (10) (2011) 969–978.

[24] J. Iturri, L. Xue, M. Kappl, L. García-Fernández, W.J.P. Barnes, H.J. Butt, A. del Campo, Torrent frog-inspired adhesives: attachment to flooded surfaces, Adv. Funct. Mater. 25 (10) (2015) 1499–1505.

[25] M. Varenberg, S.N. Gorb, Hexagonal surface micropattern for dry and wet friction, Adv. Mater. 21 (4) (2009) 483–486.

[26] T. Endlein, A. Ji, D. Samuel, N. Yao, Z. Wang, W.J. Barnes, W. Federle, M. Kappl, Z. Dai, Sticking like sticky tape: tree frogs use friction forces to enhance attachment on overhanging surfaces, J. R. Soc. Interface 10 (80) (2013) 20120838.

[27] W.M. Kier, A.M. Smith, The structure and adhesive mechanism of octopus suckers, Integr. Comp. Biol. 42 (6) (2002) 1146.

[28] F. Tramacere, L. Beccai, M. Kuba, A. Gozzi, A. Bifone, B. Mazzolai, The morphology and adhesion mechanism of Octopus vulgaris suckers, PLoS One 8 (6) (2013) e65074.

[29] S. Baik, D.W. Kim, Y. Park, T.J. Lee, S. Ho Bhang, C. Pang, A wet-tolerant adhesive patch inspired by protuberances in suction cups of octopi, Nature 546 (7658) (2017) 396–400.

[30] P. Chattopadhyay, S.K. Ghoshal, Adhesion technologies of bio-inspired climbing robots: a survey, Int. J. Robot. Autom. 33 (6) (2018).

[31] M. Zhou, Y. Tian, D. Sameoto, X. Zhang, Y. Meng, S. Wen, Controllable interfacial adhesion applied to transfer light and fragile objects by using gecko inspired mushroom-shaped pillar surface, ACS Appl. Mater. Interfaces 5 (20) (2013) 10137–10144.

[32] Y. Wang, H. Tian, J. Shao, D. Sameoto, X. Li, L. Wang, H. Hu, Y. Ding, B. Lu, Switchable dry adhesion with step-like micropillars and controllable interfacial contact, ACS Appl. Mater. Interfaces 8 (15) (2016) 10029–10037.

[33] J. Purtov, M. Frensemeier, E. Kroner, Switchable adhesion in vacuum using bio-inspired dry adhesives, ACS Appl. Mater. Interfaces 7 (43) (2015) 24127–24135.

[34] P.Y. Isla, E. Kroner, A novel bioinspired switchable adhesive with three distinct adhesive states, Adv. Funct. Mater. 25 (16) (2015) 2444–2450.

[35] M.K. Kwak, C. Pang, H.E. Jeong, H.N. Kim, H. Yoon, H.S. Jung, K.Y. Suh, Towards the next level of bioinspired dry adhesives: new designs and applications, Adv. Funct. Mater. 21 (19) (2011) 3606–3616.

[36] X. Li, D. Tao, H. Lu, P. Bai, Z. Liu, L. Ma, Y. Meng, Y. Tian, Recent developments in gecko-inspired dry adhesive surfaces from fabrication to application, Surf. Topogr. Metrol. Prop. 7 (2) (2019).

[37] G. Hanna, W.J.P. Barnes, Adhesion and detachment of the toe pads of tree frogs, J. Exp. Biol. 155 (1) (1991) 103–125.

[38] W.J. Barnes, C. Oines, J.M. Smith, Whole animal measurements of shear and adhesive forces in adult tree frogs: insights into underlying mechanisms of adhesion obtained from studying the effects of size and scale, J. Comp. Physiol. A 192 (11) (2006) 1179–1191.

[39] W.J.P. Barnes, J. Pearman, J. Platter, Application of peeling theory to tree frog adhesion, a biological system with biomimetic implications, Eur. Acad. Sci. E Newslett Sci. Technol. 1 (2008) 1–2.

[40] S. Wang, M. Li, W. Huang, X. Wang, Sticking/Climbing ability and morphology studies of the toe pads of chinese fire belly newt, J. Bionic Eng. 13 (1) (2016) 115–123.

[41] H. Dewitz, Ueber die Fortbewegung der Thiere an senkrechten, glatten Flächen vermittelst eines secretes, Arch Ges Physiol 33 (1) (1884) 440–481.

[42] H.J. Butt, M. Kappl, Normal capillary forces, Adv. Colloid Interface Sci. 146 (1–2) (2009) 48–60.

[43] F. Meng, Q. Liu, X. Wang, D. Tan, L. Xue, W.J.P. Barnes, Tree frog adhesion biomimetics: opportunities for the development of new, smart adhesives that adhere under wet conditions, Philosophical transactions, Series A, Math. Phys. Eng. Sci. 377 (2150) (2019) 20190131.

[44] M. Kappl, F. Kaveh, W.J.P. Barnes, Nanoscale friction and adhesion of tree frog toe pads, Bioinspir. Biomim. 11 (3) (2016) 035003.

[45] D.M. Drotlef, E. Appel, H. Peisker, K. Dening, A. del Campo, S.N. Gorb, W.J. P. Barnes, Morphological studies of the toe pads of the rock frog, Staurois parvus (family: Ranidae) and their relevance to the development of new biomimetically inspired reversible adhesives, Interface Focus 5 (1) (2014), 20140036-20140036.

[46] W.J. Barnes, M. Baum, H. Peisker, S.N. Gorb, Comparative Cryo-SEM and AFM studies of hylid and rhacophorid tree frog toe pads, J. Morphol. 274 (12) (2013) 1384–1396.

[47] W.-T. Chen, K. Manivannan, C.-C. Yu, J.P. Chu, J.-K. Chen, Fabrication of an artificial nanosucker device with a large area nanotube array of metallic glass, Nanoscale 10 (3) (2018) 1366–1375.

[48] J.-K. Chen, W.-T. Chen, C.-C. Cheng, C.-C. Yu, J.P. Chu, Metallic glass nanotube arrays: preparation and surface characterizations, Mater. Today 21 (2) (2018) 178–185.

[49] N. Crawford, T. Endlein, J.T. Pham, M. Riehle, W.J. Barnes, When the going gets rough - studying the effect of surface roughness on the adhesive abilities of tree frogs, Beilstein J. Nanotechnol. 7 (2016) 2116–2131.

[50] H. Chen, L. Zhang, D. Zhang, P. Zhang, Z. Han, Bioinspired surface for surgical graspers based on the strong wet friction of tree frog toe pads, ACS Appl. Mater. Interfaces 7 (25) (2015) 13987–13995.

[51] M. Li, W. Huang, X. Wang, Bioinspired, peg-studded hexagonal patterns for wetting and friction, Biointerphases 10 (3) (2015) 031008.

[52] L. Xue, B. Sanz, A. Luo, K.T. Turner, X. Wang, D. Tan, R. Zhang, H. Du, M. Steinhart, C. Mijangos, Hybrid surface patterns mimicking the design of the adhesive toe pad of tree frog, ACS Nano 11 (10) (2017) 9711–9719.

[53] D.W. Kim, S. Baik, H. Min, S. Chun, H.J. Lee, K.H. Kim, J.Y. Lee, C. Pang, Highly permeable skin patch with conductive hierarchical architectures inspired by amphibians and octopi for omnidirectionally enhanced wet adhesion, Adv. Funct. Mater. (2019).

[54] C. Greiner, A. del Campo, E. Arzt, Adhesion of bioinspired micropatterned surfaces: effects of pillar radius, aspect ratio, and preload, Langmuir 23 (7) (2007) 3495–3502.

[55] J. Xie, M. Li, Q. Dai, W. Huang, X. Wang, Key parameters of biomimetic patterned surface for wet adhesion, Int. J. Adhes. Adhes. 82 (2018) 72–78.

[56] E. Arzt, S. Gorb, R. Spolenak, From micro to nano contacts in biological attachment devices, Proc. Natl. Acad. Sci. U. S. A. 100 (19) (2003) 10603–10606.

[57] M. Li, Q. Dai, W. Huang, X. Wang, Pillar versus dimple patterned surfaces for wettability and adhesion with varying scales, J. R. Soc. Interface 15 (148) (2018).

[58] J.K.A. Langowski, D. Dodou, M. Kamperman, J.L. van Leeuwen, Tree frog attachment: mechanisms, challenges, and perspectives, Front. Zool. 15 (2018) 32.

[59] M. Li, Q. Jiao, Q. Dai, L. Shi, W. Huang, X. Wang, Effects of bulk viscoelasticity and surface wetting on the contact and adhesive properties of a soft material, Polym. Test. (2019).

[60] M. Li, J. Xie, Q. Dai, W. Huang, X. Wang, Effect of wetting case and softness on adhesion of bioinspired micropatterned surfaces, J. Mech. Behav. Biomed. Mater. 78 (00) (2018) 266–272.

[61] P. Rao, T.L. Sun, L. Chen, R. Takahashi, G. Shinohara, H. Guo, D.R. King, T. Kurokawa, J.P. Gong, Tough hydrogels with fast, strong, and reversible underwater adhesion based on a multiscale design, Adv Mater (2018) e1801884.

[62] D.M. Green, Adhesion and the toe-pads of tree frogs, Copeia 4 (1981) 790–796.

[63] M. Li, J. Xie, L. Shi, W. Huang, X. Wang, Controlling direct contact force for wet adhesion with different wedged film stabilities, J. Phys. D Appl. Phys. 51 (16) (2018) 165305.
[64] P. Martin, F. Brochard-Wyart, Dewetting at Soft interfaces, Phys. Rev. Lett. 80 (15) (1998) 3296–3299.
[65] A. Sharma, Relationship of thin film stability and morphology to macroscopic parameters of wetting in the apolar and polar systems, Langmuir 9 (3) (1993) 861–869.
[66] F.B. Wyart, J. Daillant, Drying of solids wetted by thin liquid films, Can. J. Phys. 68 (9) (1989) 1084–1088.
[67] F. Brochardwyart, J.M.D. Meglio, D. Quere, P.G.D. Gennes, Spreading of nonvolatile liquids in a continuum picture, Langmuir 7 (2) (1991) 335–338.
[68] C. Redon, F. Brochard-Wyart, F. Rondelez, Dynamics of dewetting, Phys. Rev. Lett. 66 (6) (1991) 715–718.
[69] F.B. Wyart, P. Martin, C. Redon, Liquid/liquid dewetting, Langmuir 9 (12) (1993) 3682–3690.
[70] R. Khanna, A.T.J, A. Sharma, Stability and breakup of thin polar films on coated substrates: relationship to macroscopic parameters of wetting, Ind. Eng. Chem. Res. 35 (9) (1996) 3081–3092.
[71] A. Sharma, Equilibrium contact angles and film thicknesses in the apolar and polar systems: role of intermolecular interactions in coexistence of drops with thin films, Langmuir 9 (12) (1993) 3580–3586.
[72] G.ünter Reiter†, Ashutosh Sharma, Alain Casoli, Marieodile David, A. Rajesh Khanna, P. Auroy§, Thin film instability induced by long-range forces, Langmuir 15 (7) (1999) 2551–2558.
[73] A. Martin, A. Buguin, F. Brochardwyart, Dewetting nucleation centers at Soft interfaces, Langmuir 17 (21) (2001) 6553–6559.
[74] J. Qian, J. Lin, M. Shi, Combined dry and wet adhesion between a particle and an elastic substrate, J. Colloid Interface Sci. 483 (0) (2016) 321–333.
[75] D. Maugis, B. Gauthier-Manuel, JKR-DMT transition in the presence of a liquid meniscus, J. Adhes. Sci. Technol. 8 (11) (1994) 1311–1322.
[76] D. Xu, K.M. Liechti, K. Ravi-Chandar, On the modified Tabor parameter for the JKR–DMT transition in the presence of a liquid meniscus, J. Colloid Interface Sci. 315 (2) (2007) 772–785.
[77] A.D. Roberts, D. Tabor, Surface forces: direct measurement of repulsive forces due to electrical double layers on solids, Nature 219 (5159) (1968) 1122.
[78] A.D. Roberts, P.D. Swales, The elastohydrodynamic lubrication of a highly elastic cylindrical surface, J. Phys. D Appl. Phys. 2 (09) (1969) 1317–1326.
[79] A. Roberts, Role of electrical repulsive forces in synovial fluid, Nature 231 (5303) (1971) 434–436.
[80] A.D. Roberts, The shear of thin liquid films, J. Phys. D Appl. Phys. 4 (3) (1971) 433.
[81] J.N. Israelachvili, Intermolecular and Surface Forces - Intermolecular and Surface Forces, third edition, Academic Press, 1985.
[82] K.C. Marshall, R. Stout, R. Mitchell, Mechanism of initial event in sorption of marine Bacteria to surfaces, J. Gen. Microbiol. 68 (3) (1971) 337–348.
[83] X. Zhang, X. Yi, S.I.U. Ahmed, M. Kosinskiy, Y. Liu, J.A. Schaefer, Dynamic contact model based on Meniscus adhesion for wet bio-adhesive pads: simulation experiments, Tribol. Trans. 53 (2) (2010) 280–287.
[84] Christopher D. Willett†, Michael J. Adams, A. Simon, A. Johnson, J.P.K. Seville†, Capillary bridges between two spherical bodies, Langmuir 16 (24) (2000) 9396–9405.
[85] Mahdi Farshchitabrizi, Michael Kappl, Yajun Cheng, A. Jochen Gutmann, Hansjürgen Butt, On the adhesion between fine particles and nanocontacts: an atomic force microscope study, Langmuir 22 (5) (2006) 2171.
[86] N.M. And, J.N. Israelachvili, Nanoscale mechanisms of evaporation, condensation and nucleation in confined geometries, J. Phys. Chem. B 106 (14) (2002) 3534–3537.
[87] Adam A. Feiler§, Johanna Stiernstedt, Katarina Theander, A. Paul Jenkins, Mark W. Rutland, Effect of capillary condensation on friction force and adhesion, Langmuir 23 (2) (2007) 517.
[88] M.M. Kohonen, N. Maeda, H.K. Christenson, Kinetics of capillary condensation in a nanoscale pore, Phys.rev.lett 82 (23) (1999) 4667–4670.
[89] J.B. Sokoloff, Effects of capillary forces on a hydrogel sphere pressed against a surface, Langmuir 32 (1) (2016) 135–139.
[90] B. Bhushan, Adhesion and stiction: Mechanisms, measurement techniques, and methods for reduction, J. Vac. Sci. Technol. B Microelectron. Nanometer Struct. Process. Meas. Phenom. 21 (6) (2003) 2262–2296.
[91] Y.E. Liang, Y.H. Weng, H.K. Tsao, Y.J. Sheng, Meniscus shape and wetting competition of a drop between a cone and a plane, Langmuir 32 (33) (2016) 8543–8549.
[92] L. Yang, Y.-s. Tu, H.-l. Tan, Influence of atomic force microscope (AFM) probe shape on adhesion force measured in humidity environment, Appl. Math. Mech. 35 (5) (2014) 567–574.
[93] S.H. Chen, A.K. Soh, The capillary force in micro- and nano-indentation with different indenter shapes, Int. J. Solids Struct. 45 (10) (2008) 3122–3137.
[94] E.J.D. Souza, M. Brinkmann, C. Mohrdieck, E. Arzt, Enhancement of capillary forces by multiple liquid bridges, Langmuir 24 (16) (2008) 8813–8820.
[95] E.J.D. Souza, M. Brinkmann, C. Mohrdieck, A. Crosby, E. Arzt, Capillary forces between chemically different substrates, Langmuir 24 (18) (2008) 10161–10168.
[96] S. Cai, B. Bhushan, Meniscus and viscous forces during separation of hydrophilic and hydrophobic surfaces with liquid-mediated contacts, Mater. Sci. Eng. R Rep. 61 (1–6) (2008) 78–106.
[97] H. Chen, A. Amirfazli, T. Tang, Modeling liquid bridge between surfaces with contact angle hysteresis, Langmuir 29 (10) (2013) 3310–3319.
[98] F. Restagno, C. Poulard, C. Cohen, L. Vagharchakian, L. Leger, Contact angle and contact angle hysteresis measurements using the capillary bridge technique, Langmuir 25 (18) (2009) 11188–11196.
[99] E.J. De Souza, L. Gao, T.J. Mccarthy, E. Arzt, A.J. Crosby, Effect of contact angle hysteresis on the measurement of capillary forces, Langmuir 24 (4) (2008) 1391–1396.
[100] S. Reddy, E. Arzt, A. del Campo, Bioinspired surfaces with switchable adhesion, Adv. Mater. 19 (22) (2007) 3833–3837.
[101] J. Cui, D.M. Drotlef, I. Larraza, J.P. Fernandez-Blazquez, L.F. Boesel, C. Ohm, M. Mezger, R. Zentel, A. del Campo, Bioinspired actuated adhesive patterns of liquid crystalline elastomers, Adv. Mater. 24 (34) (2012) 4601–4604.
[102] M. Frensemeier, J.S. Kaiser, C.P. Frick, A.S. Schneider, E. Arzt, R.S. Fertig, E. Kroner, Temperature-induced switchable adhesion using nickel-titanium-Polydimethylsiloxane hybrid surfaces, Adv. Funct. Mater. 25 (20) (2015) 3013–3021.
[103] D.M. Drotlef, P. Blumler, A. del Campo, Magnetically actuated patterns for bioinspired reversible adhesion (dry and wet), Adv. Mater. 26 (5) (2014) 775–779.
[104] F.K.A. Chiao, Fabrication and patterning of magnetic polymer micropillar structures using a dry-nanoparticle embedding technique, J. Microelectromech. Syst. (2013).
[105] M. Li, Q. Dai, Q. Jiao, W. Huang, X. Wang, Magnetically stimulating capillary effect for reversible wet adhesions, Soft Matter (2019).
[106] V. Bashtovoi, P. Kuzhir, A. Reks, Capillary ascension of magnetic fluids, J. Magn. Magn. Mater. 252 (252) (2002) 265–267.
[107] V. Bashtovoi, G. Bossis, P. Kuzhir, A. Reks, Magnetic field effect on capillary rise of magnetic fluids, J. Magn. Magn. Mater. 289 (0) (2005) 376–378.
[108] Z. Wang, Z. Hu, W. Huang, X. Wang, Elastic support of magnetic fluids bearing, J. Phys. D Appl. Phys. 50 (43) (2017) 435004.